Journal of Molecular Spectroscopy **211,** 235–240 (2002)
doi:10.1006/jmsp.2001.8468, available online at http://www.idealibrary.com on IDEAL®

Carbon-13 Isotopic Species of H_2C_3, H_2C_4, and H_2C_5: High-Resolution Rotational Spectra

M. C. McCarthy and P. Thaddeus

Harvard–Smithsonian Center for Astrophysics, 60 Garden Street, Cambridge, Massachusetts 02138; and Division of Engineering and Applied Sciences, Harvard University, 29 Oxford Street, Cambridge, Massachusetts 02138

Received July 26, 2001; in revised form October 3, 2001

The microwave rotational spectra of the carbon-13 isotopic species of H_2C_3, H_2C_4, and H_2C_5 have been observed in a pulsed supersonic molecular beam by Fourier transform microwave spectroscopy. At high resolution all of the rotational lines exhibit hyperfine structure produced by the magnetic interaction between the nuclear spin of ^{13}C and the overall rotation of the molecule. The component of the nuclear spin–rotation tensor along the a-inertial axis is large for most isotopic species, especially at the carbene carbon; at this position C_{aa} is two to three times larger than at other substituted positions along the chain. In contrast to both H_2C_3 and H_2C_3, in H_2C_4 C_{aa} exhibits a pronounced alternation along the carbon chain backbone. Following detection of the five carbon-13 isotopic species and D_2C_5, an experimental structure (r_0) has been determined to high accuracy for H_2C_5.

I. INTRODUCTION

The cumulene carbenes $H_2CC_n=C$: are well-known laboratory and astronomical molecules. In space, H_2C_3, H_2C_4, and H_2C_6 have been observed with radio telescopes (*1–5*) in the molecular envelope of the carbon-rich star IRC + 10216, in the cold dark cloud TMC-1, or in both locations. Longer molecules of the series to H_2C_9 and D_2C_{10} have been characterized spectroscopically in this laboratory by Fourier transform microwave (FTM) spectroscopy of a supersonic molecular beam (*6*). From rotational spectroscopy of the carbon-13 and deuterium isotopic species, experimental structures have been derived for both H_2C_3 (*7*) and H_2C_4 (*8*). The work here on H_2C_3 and its isotopic species was done at millimeter wavelengths at a spectral resolution of about 2–3 ppm (500 kHz FWHM), and that on H_2C_4 and its isotopic species was done at centimeter wavelengths with a FTM spectrometer at comparable resolution, 2 ppm (50 kHz FWHM), using a molecular beam perpendicular to the axis of the Fabry–Perot cavity.

The present study was motivated by the FTM detection of the silacumulene chain H_2CCSi and its rare isotopic species, described in the accompanying paper (*9*). Because lines only about 5 kHz wide (i.e., a spectral resolution of 0.2 ppm) are routinely observed when FTM spectroscopy is used in combination with an axial molecular beam (*10*), it was possible to detect in the silicon-29 and the two single carbon-13 isotopic species of H_2CCSi well-resolved hyperfine structure (hfs) from the spin–rotation interaction between the nuclear spin and the weak molecular magnetic field induced by rotation. To see if comparable hfs can be detected in other cumulenic chains with two equivalent protons and C_{2v} symmetry, a systematic investigation of the rotational spectra of the carbon-13 isotopic species of several such carbenes was therefore undertaken. Chains such as H_2C_3 and H_2C_4 are convenient systems for study because they are readily produced in our discharge source and because spectroscopic constants for their singly substituted isotopic species have been determined (*7, 8*).

We present here high-resolution rotational spectra of the carbon-13 isotopic species of three cumulene carbenes: H_2C_3, H_2C_4, and H_2C_5. At high resolution, it has been possible to detect hfs in all of the single carbon-13 species and to determine the component of the nuclear spin-rotation tensor along each inertial axis. As in H_2CCSi, the component along the a-inertial axis, C_{aa}, is largest at the carbene carbon, owing to the pair of singlet-coupled electrons located on this terminal atom. Although C_{aa} is otherwise fairly constant along the carbon chain in both H_2C_3 and H_2C_5, in H_2C_4 a pronounced alternation is observed, and at two of the remaining three carbon positions, C_{aa} is small. From the rotational constants of carbon-13 and the D_2C_5 isotopic species, a fairly good experimental (r_0) structure has been determined for H_2C_5.

II. EXPERIMENTAL

Rotational lines of the carbon-13 isotopic species of the three carbenes here were detected with the same FTM spectrometer and discharge source used to study H_2CCSi, H_2C_4Si (*9*), and the four silicon–sulfur chains SiC_2S, SiC_3S, SiC_4S, and SiC_6S (*11*). For H_2C_3 and H_2C_4, the isotopic species were detected in natural abundance using the same gas mixture and source conditions previously used for H_2C_7 and longer cumulene carbenes up to H_2C_9 (*6*): a discharge through a mixture of 0.25% diacetylene (HC_4H) in neon, a gas pulse of duration 200 μsec (15–20 sccm flow), a 1000 V dc discharge applied in the throat

0022-2852/02 $35.00

of the supersonic nozzle, and a nozzle backing pressure of 2.5 kTorr (3.2 atm). To detect the isotopic species of H_2C_5, a statistical mixture of carbon-13 HCCH (25% HCCH, 50% $H^{13}CCH$, and 25% $H^{13}C^{13}CH$) was mixed with normal HC_4H, the optimal mixture being 0.1% carbon-13 HCCH and 0.25% HC_4H in neon. Rotational lines of the five ^{13}C isotopic species were then about four times stronger than when produced in natural abundance with diacetylene alone (and were about equal in strength, to one another with no evidence of fractionation). The statistical mixture of carbon-13 HCCH was produced by the hydrolysis of ^{13}C-enriched Li_2C_2 obtained from the NIH Stable Isotope Resource, Los Alamos National Laboratory.

Although precise rotational and centrifugal distortion constants are already available for both H_2C_3 and H_2C_4 and their isotopic species, the present study is the first experimental investigation of the rotational spectra of the carbon-13 isotopic species of H_2C_5. Searches for the rotational lines were based on a high-level coupled cluster calculation of Botschwina (*12*). For each isotopic species, rotational constants calculated from the theoretical structure were scaled by the ratio of the experimental rotational constant to that calculated for the normal species. Such scaling predicts the frequencies of the isotopic lines to better than 1% of the frequency shift from lines of the normal species; a search for example of only a few MHz was required to find the $J = 3 \rightarrow 2$ transitions at 13 GHz.

III. DATA AND ANALYSIS

The measured carbon-13 hfs of the three carbenes here is given in Tables 1–3. At least two transitions for each chain were measured in both the $K_a = 0$ and $K_a = \pm 1$ rotational ladders. Additional hyperfine structure from the two equivalent hydrogen atoms was also observed in some spectra, but this is generally quite small (<10 kHz) and partially blended or unresolved at our instrumental resolution; it was therefore neglected in the present analysis.

The spectra were analyzed with Watson's S-reduced Hamiltonian, which well reproduces the observed spectra with at most seven spectroscopic parameters: the two rotational constants, B and C, the two leading centrifugal distortion constants, D_J and D_{JK}, and the three diagonal elements of the nuclear spin–rotation tensor, C_{aa}, C_{bb}, and C_{cc}, where the Hamiltonian for the hyperfine interaction is given by

$$H_{hfs} = C_{aa}J_aI_a + C_{bb}J_bI_b + C_{cc}J_cI_c.$$

The rotational and centrifugal distortion constants are summarized in Table 4; the spin–rotation constants are given in Table 5. For the H_2C_3 and H_2C_4 isotopic species, the A rotational constant was constrained to the value previously determined from the millimeter-wave data; for H_2C_5, A was constrained to the value of the normal species. For many of the isotopic species, owing to the lack of resolved hfs in the $K_a = 0$ ladder, the C_{bb} and C_{cc} tensor elements were constrained to zero (see Fig. 1). The rotational and centrifugal distortion constants determined here for the isotopic species of H_2C_3 and H_2C_4 are in excellent agreement with previously reported values (*7, 8*).

TABLE 1
Microwave Transitions of the H_2C_3 Isotopic Species (in MHz)

$J'_{K_a,K_c} \rightarrow J''_{K_a,K_c}$	$F' \rightarrow F''$	$H_2{}^{13}CCC$	$H_2C^{13}CC$	$H_2CC^{13}C$
$1_{0,1} \rightarrow 0_{0,0}$	$3/2 \rightarrow 1/2$	20194.442	20785.161	20004.507
	$1/2 \rightarrow 1/2$		20785.153	20004.492
$2_{1,2} \rightarrow 1_{1,1}$	$5/2 \rightarrow 3/2$	40024.021	41183.952	39650.837
	$3/2 \rightarrow 1/2$	40024.074	41184.002	39650.956
$2_{0,2} \rightarrow 1_{0,1}$	$5/2 \rightarrow 3/2$	40388.434	41569.819	40008.577
	$3/2 \rightarrow 1/2$			40008.561
$2_{1,1} \rightarrow 1_{1,0}$	$5/2 \rightarrow 3/2$	40749.638	41953.350	40364.050
	$3/2 \rightarrow 1/2$	40749.689	41953.398	40364.164

Note. Experimental uncertainties (1σ) are 2 kHz. Observed minus calculated frequencies are 0–2 kHz; the best-fit constants are given in Table 4 and 5.

IV. THE STRUCTURE OF H_2C_5

An experimental (r_0) structure (*13*) of H_2C_5 was obtained by a least-squares adjustment of the five bonds and the HCH bond angle in Fig. 2 to reproduce the measured rotational constants in Table 4 (i.e., those of the five rare isotopic species and D_2C_5, plus the normal, on the assumption that H_2C_5 is planar and possess C_{2v} symmetry). Uncertainties in the bond lengths and the bond angle were derived on the assumption that the largest source of error is zero point vibration. The uncertainty in the rotational constants which yields a χ^2 of 8, the most probable value for eight degrees of freedom (*14*), is $\Delta B = 0.06$ MHz. Although a substitution structure (r_s) could also be derived from the available data, we have chosen not to report it here because of the large uncertainties for the central bond lengths.

The r_0 structure is compared in Table 6 with an equilibrium r_e structure of H_2C_5 calculated *ab initio* at the coupled cluster level of theory (*12*). With the exception of the C–H bond, all bonds agree with those calculated to better than 0.008 Å. Because of the light mass of the hydrogen atoms and because the A rotational constant was not determinable for any of the isotopic species, it is not surprising that the C–H bond differs from that calculated by more than that, or that the ∠HCH angle is larger than that calculated by 1°–2°. As in H_2C_3 and H_2C_4, the CC bonds in H_2C_5 are fairly uniform and close in length to those of typical double bonds—evidence that the bonding is cumulenic along the carbon chain backbone.

V. DISCUSSION

All three carbenes have large spin–rotation coupling constants for most of their carbon nuclei. As in H_2CCSi(*9*), C_{aa} is large because this constant is proportional to the A rotational constant,

TABLE 2
Microwave Transitions of the H_2C_4 Isotopic Species (in MHz)

$J'_{K_a,K_c} \rightarrow J''_{K_a,K_c}$	$F' \rightarrow F''$	$H_2{}^{13}CCCC$	$H_2C^{13}CCC$	$H_2CC^{13}CC$[a]	$H_2CCC^{13}C$
$1_{0,1} \rightarrow 0_{0,0}$	$3/2 \rightarrow 1/2$	8675.462	8909.542	8887.701	8621.768
	$1/2 \rightarrow 1/2$				8621.758
$2_{1,2} \rightarrow 1_{1,1}$	$5/2 \rightarrow 3/2$	17279.928	17744.186	17700.845	17173.355
	$3/2 \rightarrow 1/2$	17279.941	17744.230		17173.423
$2_{0,2} \rightarrow 1_{0,1}$	$5/2 \rightarrow 3/2$	17350.898	17819.057	17775.368	17243.508
	$3/2 \rightarrow 1/2$				
$2_{1,1} \rightarrow 1_{1,0}$	$5/2 \rightarrow 3/2$	17420.838	17892.815	17848.811	17312.595
	$3/2 \rightarrow 1/2$	17420.850	17892.854		17312.660
$3_{1,3} \rightarrow 2_{1,2}$	$7/2 \rightarrow 5/2$	25919.854	26616.248	26551.227	25760.008
	$5/2 \rightarrow 3/2$		26616.269		25760.031
$3_{0,3} \rightarrow 2_{0,2}$	$7/2 \rightarrow 5/2$	....	26728.514	26662.982	25865.196
	$5/2 \rightarrow 3/2$	....			
$3_{1,2} \rightarrow 2_{1,1}$	$7/2 \rightarrow 5/2$	26131.222	26839.193	26773.180	25968.868
	$5/2 \rightarrow 3/2$		26839.207		25968.894

Note. Experimental uncertainties (1σ) are 2 kHz. Observed minus calculated frequencies are 0–2 kHz; the best-fit constants are given in Table 4 and 5.

[a] Centroid of hyperfine-split lines is given owing to comparable carbon-13 and hydrogen hfs.

TABLE 3
Microwave Transitions of the H_2C_5 Isotopic Species (in MHz)

$J'_{K_a,K_c} \rightarrow J''_{K_a,K_c}$	$F' \rightarrow F''$	$H_2{}^{13}CCCCC$	$H_2C^{13}CCCC$	$H_2CC^{13}CCC$	$H_2CCC^{13}CC$	$H_2CCCC^{13}C$
$3_{1,3} \rightarrow 2_{1,2}$	$7/2 \rightarrow 5/2$	13371.775	13659.257	13742.350	13623.626	13315.067
	$5/2 \rightarrow 3/2$	13371.968	13659.279	13742.378	13623.649	13315.119
$3_{0,3} \rightarrow 2_{0,2}$	$7/2 \rightarrow 5/2$	13399.155	13687.664	13771.102	13651.868	13342.059
	$5/2 \rightarrow 3/2$					
$3_{1,2} \rightarrow 2_{1,1}$	$7/2 \rightarrow 5/2$	13425.830	13715.511	13799.283	13679.554	13368.497
	$5/2 \rightarrow 3/2$	13425.856	13715.532	13799.312	13679.576	13368.552
$4_{1,4} \rightarrow 3_{1,3}$	$9/2 \rightarrow 7/2$	17829.254	18212.334	18323.126	18164.826	17753.423
	$7/2 \rightarrow 5/2$	17829.267	18212.346	18323.144	18164.842	17753.450
$4_{0,4} \rightarrow 3_{0,3}$	$9/2 \rightarrow 7/2$	17865.524	18250.202	18361.452	18202.475	17789.400
	$7/2 \rightarrow 5/2$					
$4_{1,3} \rightarrow 3_{1,2}$	$9/2 \rightarrow 7/2$	17901.101	18287.339	18399.039	....	17824.666
	$7/2 \rightarrow 5/2$	17901.113	18287.354	18399.057	....	17824.692
$5_{0,5} \rightarrow 4_{0,4}$	$11/2 \rightarrow 9/2$	....	....	....	....	22236.723
	$9/2 \rightarrow 7/2$	....	....	....	....	

Note. Experimental uncertainties (1σ) are 2 kHz. Observed minus calculated frequencies are 0–2 kHz; the best-fit constants are given in Table 4 and 5.

TABLE 4
Rotational and Centrifugal Distortion Constants for the Carbon-13 Isotopic Species of H_2C_3, H_2C_4, and H_2C_5 (in MHz)

Isotopic Species	A	B	C	$D_J \times 10^3$	D_{JK}
$H_2{}^{13}CCC$	288800[a]	10278.6330(1)	9915.8250(1)	4.0(2)	0.4864(6)
$H_2C^{13}CC$	288610[a]	10584.9379(1)	10200.238(1)	4.1(2)	0.3890(13)
$H_2CC^{13}C$	288860[a]	10180.561(1)	9823.956(1)	3.9(2)	0.3602(9)
$H_2{}^{13}CCCC$	284468[b]	4372.960(6)	4302.5046(6)	0.56(4)	0.1313(5)
$H_2C^{13}CCC$	284468[b]	4491.9286(5)	4417.6150(5)	0.52(3)	0.1398(3)
$H_2CC^{13}CC$	284468[b]	4480.8419(6)	4406.8580(6)	0.54(3)	0.1383(3)
$H_2CCC^{13}C$	284468[b]	4345.6940(5)	4276.0739(5)	0.51(3)	0.1324(3)
$H_2{}^{13}CCCCC$	275322[c]	2242.1758(4)	2224.2142(4)	0.107(12)	0.0436(2)
$H_2C^{13}CCCC$	275322[c]	2290.6556(5)	2271.9041(5)	0.106(14)	0.0460(2)
$H_2CC^{13}CCC$	275322[c]	2304.6750(5)	2285.6969(5)	0.097(13)	0.0464(2)
$H_2CCC^{13}CC$	275322[c]	2284.6350(5)	2265.9925(7)	0.100(17)	0.0456(3)
$H_2CCCC^{13}C$	275322[c]	2232.5842(5)	2214.7736(5)	0.098(9)	0.0438(2)

Note. The 1σ uncertainties (in parentheses) are in the last significant digit.

[a] From Ref. *7*.

[b] From Ref. *8*.

[c] From Ref. *22*.

TABLE 5
Diagonal Elements of the Spin–Rotation Tensor for the Carbon-13 Isotopic Species of H_2C_3, H_2C_4, and H_2C_5 (in kHz)

Isotopic Species	C_{aa}	C_{bb}	C_{cc}
$H_2{}^{13}CCC$	152(6)	....	....
$H_2C^{13}CC$	168(10)	7(4)	3(4)
$H_2CC^{13}C$	391(9)	15(4)	5(4)
$H_2{}^{13}CCCC$	38(6)	....	....
$H_2C^{13}CCC$	125(6)	....	....
$H_2CC^{13}CC$	<25[a]	....	....
$H_2CCC^{13}C$	226(9)	....	....
$H_2{}^{13}CCCCC$	185(14)	....	....
$H_2C^{13}CCCC$	179(14)	....	....
$H_2CC^{13}CCC$	237(14)	....	....
$H_2CCC^{13}CC$	188(15)	....	....
$H_2CCCC^{13}C$	422(14)	6(3)	6(3)

Note. The 1σ uncertainties (in parentheses) are in the last significant digit.

[a] Owing to the strong blend of carbon-13 and hydrogen hfs, only an upper limit of C_{aa} is possible.

which is nearly 10 cm^{-1} in these nearly prolate, asymmetric top chains; C_{aa} has been determined to an accuracy of about 5% for most of the present isotopic species, and as Fig. 2 shows, considerable variations in the magnitude of C_{aa} are observed, even between adjacent atoms along the carbon chain. The C_{aa} values determined here are larger by a factor of 2 or more than those reported for carbon-13 substituted formaldehyde [$C_{aa} = 127.86(31)$ kHz; Ref. (*15*)] or ketene [$H_2C^{13}CO$: $C_{aa} = 71(8)$ kHz; Ref. (*16*)].

The theory of nuclear spin–rotation is summarized in the accompanying paper on the rotational spectroscopy of H_2CCSi and H_2C_4Si (*9*). Carbon-13 isotopic substitution presumably has a negligible effect on excited state energies, on the radial and angular distribution of valence electrons, or on the A rotational constant. The ratio of C_{aa} for different nuclei along the chain is determined by the ratio of the average expectation value $\langle r^{-3}\rangle$ of the valence electrons in the vicinity of each, i.e., $C_{aa}^m/C_{aa}^n \propto \langle r^{-3}\rangle_m/\langle r^{-3}\rangle_n$, where m, n denote the various carbon atoms. For this reason, experimental determinations of spin–rotation coupling constants may provide a sensitive probe of the electronic structure of the carbene; they also may provide stringent tests for theory because these constants should ultimately be calculable *ab initio* from the molecular structure.

The diagonal element C_{aa} of the nuclear spin–rotation tensor is largest (by a factor of 2 or more) at the carbene carbon in each chain here. This finding agrees well with the prediction of valence bond theory that the two nonbonding electrons are

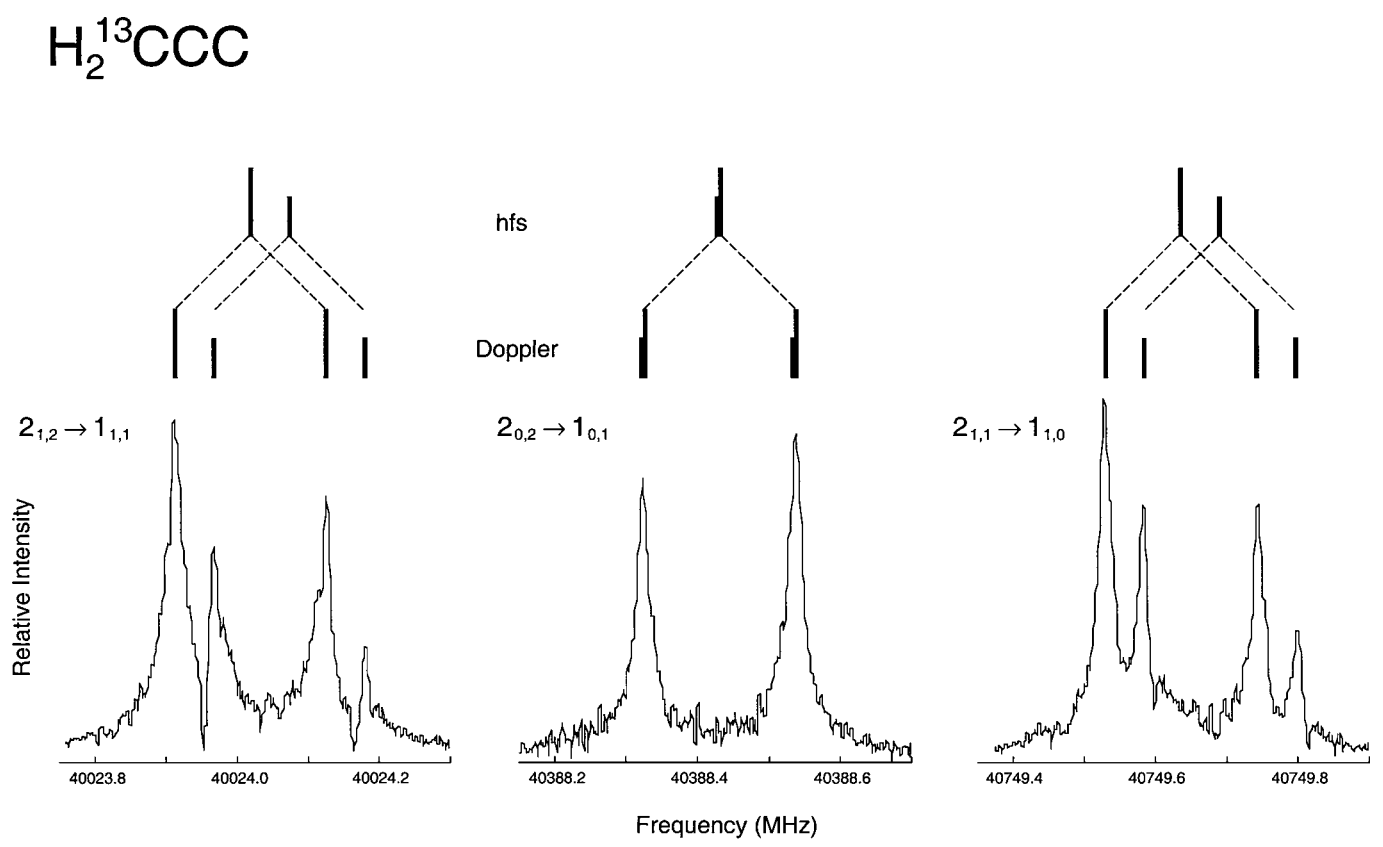

FIG. 1. Sample spectra of $H_2{}^{13}CCC$ showing spin–rotation hfs in rotational transitions near 40.5 GHz in the $K_a = 0$ and the two $K_a = \pm 1$ rotational ladders. Each hyperfine transition has a double-peaked line profile as a result of the interaction between the fast moving molecular beam and the two traveling waves that compose the confocal Fabry–Perot mode. Typical integration times were 3 min per spectrum.

TABLE 6
H_2C_5 Structures

Parameter	Experimental (r_0)	Theoretical CASSCF[a] 6-31G**	Theoretical MP2[a] 6-31G**	Theoretical CCSD(T)[b] 168 cGTO
r(H-$C_{(1)}$)/Å	1.099(1)	1.076	1.084	1.0806
r($C_{(1)}$-$C_{(2)}$)/Å	1.320(1)	1.334	1.328	1.3221
r($C_{(2)}$-$C_{(3)}$)/Å	1.263(1)	1.267	1.270	1.2656
r($C_{(3)}$-$C_{(4)}$)/Å	1.306(1)	1.302	1.309	1.2988
r($C_{(4)}$-$C_{(5)}$)/Å	1.281(1)	1.288	1.290	1.2879
∠$HC_{(1)}H$/(deg)	119.19(2)	118.07	117.08	117.98

Note. Structure that best reproduces the observed rotational transitions of the five isotopic species (see Section IV). Estimated uncertainties in the last significant digit are given in parentheses.

[a] From Ref. (*23*).

[b] From P. Botschwina (unpublished); all electrons correlated.

localized on the terminal carbon atom. The small C_{aa} of H_2C_4 relative to that of H_2C_3 of H_2C_5 presumably reflects differences in the excited state energies for cumulene chains with an even and odd number of carbon atoms.

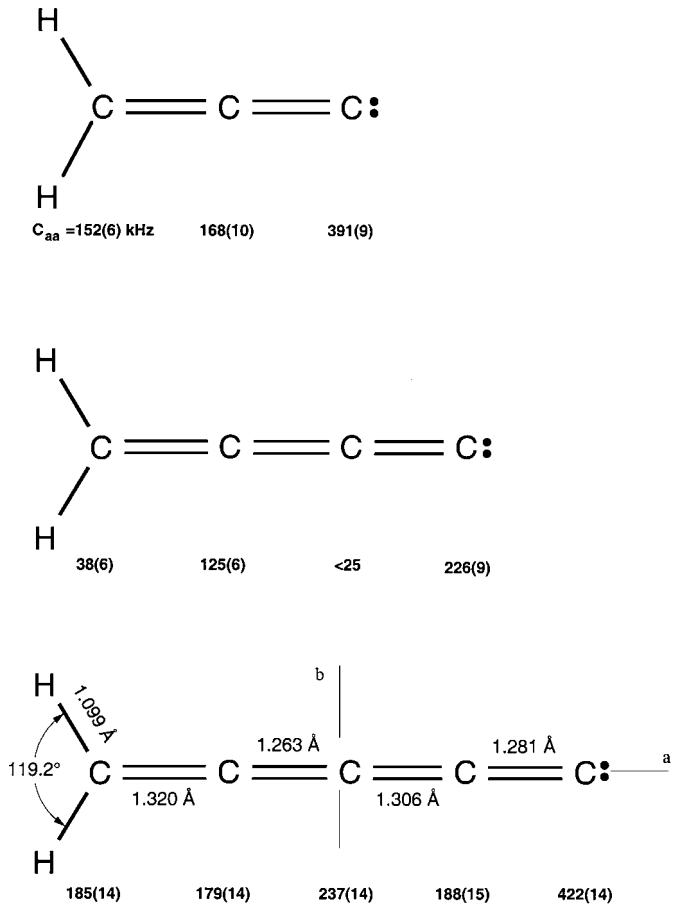

FIG. 2. Hyperfine constants of the present carbenes and the geometrical structure of H_2C_5 derived from the present data. Shown beneath each carbon atom is the spin–rotation coupling constant C_{aa}; 1σ uncertainties in the last significant digit are given in parentheses. The bond lengths and angle of H_2C_5 were obtained by isotopic substitution (see Section IV).

For H_2C_3 and H_2C_5, C_{aa} is fairly constant at each of the remaining carbon atoms, including that bonded to the terminal hydrogen atoms, a regularity which indicates that the average electron density is otherwise fairly uniform along the body of these two chains. For H_2C_4, however, C_{aa} is very small ($C_{aa} <$ 40 kHz) at two of the remaining three carbon positions, and there is a clear variation of C_{aa}. One possible explanation is that orbital excitation is fairly specific in H_2C_4 owing to differences in the overlap of the ground and excited state molecular orbitals. From a study of the carbon-13 isotopic species of H_2C_6, it would be interesting to see if this variation holds for longer cumulene chains with an even number of carbon atoms. With slight improvements in detection sensitivity, such a study should be possible with our present FTM spectrometer. An *ab initio* theoretical investigation of the spin–rotation hfs of the cumulene carbenes would also be interesting and should not be too difficult (*17–19*).

A byproduct of the present investigation is that very accurate rest frequencies are now available for the lowest-frequency transitions of the ^{13}C isotopic species for the cumulene carbenes here. H_2C_3, for example, is sufficiently intense in warm sources such as the star-forming region W51 (*20*) and the molecular envelope of the evolved carbon star IRC + 10216 (*21*) that all three ^{13}C isotopic species have been detected with radio telescopes. With the spectroscopic constants in Table 4, the astronomically most interesting lines in the radio spectrum of each can be predicted to an uncertainty of better than 1 km s^{-1} in equivalent radial velocity at frequencies as high as 80 GHz—adequate for observation in all cold molecular sources.

ACKNOWLEDGMENTS

We thank C. A. Gottlieb, J. K. G. Watson, and J. M. Brown for helpful discussions, P. Botschwina for communicating the results of his *ab initio* calculations prior to publication, J. Dudek for assistance with the synthesis of diacetylene, and E. S. Palmer for help with the microwave electronics and cryogenic system. We also gratefully acknowledge L. A. Silks III of the NIH Stable Isotope Resource at the Los Alamos National Laboratory for assistance in the production of the carbon-13 enriched lithium carbide. The Los Alamos Isotope Resource was supported by USPHS Grant RR02231 and by the U.S. Department of Energy.

The present research is supported by NASA Grant NAG5-9379 and NSF Grant AST-9820722.

REFERENCES

1. J. Cernicharo, C. A. Gottlieb, M. Guélin, T. C. Killian, G. Paubert, P. Thaddeus, and J. M. Vrtliek, *Astrophys. J. Lett.* **368,** L39–L41 (1991).
2. J. Cernicharo, C. A. Gottlieb, M. Guélin, T. C. Killian, P. Thaddeus, and J. M. Vrtliek, *Astrophys. J. Lett.* **368,** L43–L45 (1991).
3. K. Kawaguchi, N. Kaifu, M. Ohishi, S. Ishikawa, Y. Hirahara, S. Yamamoto, S. Saito, S. Takano, A. Murakami, J. M. Vrtliek, C. A. Gottlieb, P. Thaddeus, and W. M. Irvine, *Publ. Astron. Soc. Jpn.* **43,** 607–619 (1991).
4. W. D. Langer, T. Velusamy, T. B. H. Kuiper, and R. Peng, M. C. McCarthy, M. J. Travers, A. Kovács, C. A. Gottlieb, and P. Thaddeus, *Astrophys. J. Lett.* **480,** L63–L66 (1997).
5. M. Guélin, S. Muller, J. Cernicharo, A. J. Apponi, M. C. McCarthy, C. A. Gottlieb, and P. Thaddeus, *Astrophys. Astron.* **363,** L9–L12 (2000).
6. A. J. Apponi, M. C. McCarthy, C. A. Gottlieb, and P. Thaddeus, *Astrophys. J. Lett.* **530,** 357–361 (2000).
7. C. A. Gottlieb, T. C. Killian, P. Thaddeus, P. Botshwina, J. Flügge, and M. Oswald, *J. Chem. Phys.* **98,** 4478–4485 (1993).
8. M. J. Travers, W. Chen, S. E. Novick, J. M. Vrtliek, C. A. Gottlieb, and P. Thaddeus, *J. Mol. Spectrosc.* **180,** 75–80 (1996).
9. M. C. McCarthy and P. Thaddeus, *J. Mol. Spectrosc.* **211,** 228–234 (2002).
10. J.-U. Grabow and W. Stahl, *Z. Naturforsch.* **45,** 1043–1044 (1990).
11. P. Botschwina, M. Engenia Sanz, M. C. McCarthy, and P. Thaddeus, *J. Chem. Phys.*, submitted.
12. P. Botschwina, unpublished (1996).
13. M. C. McCarthy, E. S. Levine, A. J. Apponi, and P. Thaddeus, *J. Mol. Spectrosc.* **203,** 75–81 (2000).
14. W. H. Press, B. P. Flannery, S. A. Teukolsky, and W. T. Vetterling, "Numerical Recipes in C," p. 655, Cambridge, Univ. Press, Cambridge, UK, 1988.
15. K. D. Tucker, G. R. Tomasevich, and P. Thaddeus, *Astrophys. J.* **169,** 429–440 (1971).
16. R. D. Brown, P. D. Godfrey, D. McNaughton, A. P. Pierlot, W. H. Taylor, *J. Mol. Spectrosc.* **140,** 340–352 (1990).
17. J. W. Kenney, III, J. Simons, G. D. Purvis, and R. J. Bartlett, *J. Am. Chem. Soc.* **100,** 6930–6936 (1978).
18. C. E. Dykstra, C. A. Parsons, and C. L. Oates, *J. Am. Chem. Soc.* **101,** 1962–1965 (1979).
19. G. Fischer and J. P. Maier, *Chem. Phys.* **223,** 149–158 (1997).
20. M. B. Bell, L. W. Avery, and J. K. G. Watson, *Astrophys. J. Suppl. Ser.* **86,** 211–233 (1993).
21. J. Cernicharo, M. Guélin, and C. Kahane, *Astrophys. J. Suppl. Ser.* **142,** 181–215 (2000).
22. M. C. McCarthy, M. J. Travers, A. Kovács, W. Chen, S. E. Novick, C. A. Gottlieb, and P. Thaddeus, *Science* **275,** 518–520 (1997).
23. S. A. Maluendes and A. D. McLean, *Chem. Phys. Lett.* **200,** 511–517 (1992).